On the ambiguity of the reaction rate constants in multivariate curve resolution for reversible first-order reaction systems.

Henning Schröder[a], Mathias Sawall[a], Christoph Kubis[b], Detlef Selent[b], Dieter Hess[c], Robert Franke[c,d], Armin Börner[b], Klaus Neymeyr[a,b]

[a] *Universität Rostock, Institut für Mathematik, Ulmenstrasse 69, 18057 Rostock, Germany*
[b] *Leibniz-Institut für Katalyse, Albert-Einstein-Strasse 29a, 18059 Rostock, Germany*
[c] *Evonik Performance Materials GmbH, Paul-Baumann Strasse 1, 45772 Marl, Germany*
[d] *Lehrstuhl für Theoretische Chemie, Ruhr-Universität Bochum, 44780 Bochum, Germany*

Abstract

If for a chemical reaction with a known reaction mechanism the concentration profiles are accessible only for certain species, e.g. only for the main product, then often the reaction rate constants cannot uniquely be determined from the concentration data. This is a well-known fact which includes the so-called slow-fast ambiguity.

This work combines the question of unique or non-unique reaction rate constants with factor analytic methods of chemometrics. The idea is to reduce the rotational ambiguity of pure component factorizations by considering only those concentration factors which are possible solutions of the kinetic equations for a properly adapted set of reaction rate constants. The resulting set of reaction rate constants corresponds to those solutions of the rate equations which appear as feasible factors in a pure component factorization.

The new analysis of the ambiguity of reaction rate constants extends recent research activities on the Area of Feasible Solutions (AFS). The consistency with a given chemical reaction scheme is shown to be a valuable tool in order to reduce the AFS. The new methods are applied to model and experimental data.

Key words: spectral recovery, factor analysis, nonnegative matrix factorization, kinetic modeling, feasible rate constants, area of feasible solutions.

1. Introduction

Multivariate curve resolution techniques are well-established and powerful tools to extract pure component information from spectroscopic data. Unfortunately, these methods suffer from the non-uniqueness of the possible nonnegative factorizations. Usually a continuum of factorizations exists. This fact is well-known under the keyword of rotational ambiguity [1, 2]. If additionally soft- and/or hard-constraints are imposed on the solutions, then one can determine a unique solution. In general, the non-uniqueness of the nonnegative factorizations can be represented by drawing the sets of all possible concentration profiles or all possible spectra in the form of feasible bands [3]. Alternatively, the area of feasible solutions (AFS) [4, 5, 6, 7, 8, 9] is a low-dimensional representation of the set of all nonnegative concentration profiles and all nonnegative pure component spectra which appear in possible factorizations of the spectral data matrix. In this sense, we consider the AFS methodology as a *global approach* since it provides an overview of the full range of all nonnegative factorizations. In recent works [10, 11, 12] various soft constraints have directly been applied to the AFS in order to reduce the rotational ambiguity. This reduction of the ambiguity is reflected by drastically smaller subsets of the original AFS. These subsets represent the possible factorizations which additionally meet the soft constraints.

In this work the global approach including the subsequent reduction step is extended to kinetic hard-models. A kinetic hard-model is well-known to be a very powerful restriction for a multivariate curve resolution method [13, 14, 1, 15]. The parameters of such kinetic models, namely the reaction rate constants, have not to be known in advance, but can be computed during the model-fitting process by means of an optimization procedure. It is a well-known fact [16, 14, 17, 18] that sometimes the reaction rate constants cannot uniquely be determined from incomplete concentration data, e.g. if the concentration values are only accessible for the main

product of the reaction. This is a possible situation if, e.g., an isolated spectral peak of the main product can be used to extract the concentration information, see [15]. For first-order consecutive chemical reactions the non-uniqueness is also known as the "slow-fast ambiguity". In case of the slow-fast ambiguity for instance, the concentration profile of the main reaction product depends in a symmetric way on two of the reaction rate constants. In other words, these two rate constants can be permuted without changing the time-dependent concentration function of this chemical component. Possibly but not necessarily this change can be associated with negative entries in the spectral factor; this issue is also discussed in this paper. A general analysis of these questions is given in [19, 20], where identifiability and distinguishability for first-order and more general systems are the key concepts. Identifiability means that kinetic parameters for an assumed kinetic can be found in a unique way and distinguishability implies that one can determine a unique reaction scheme.

The aim of this paper is to combine the question of unique or non-unique reaction rate constants with model-free curve resolution methods for the case of general first-order kinetics. The rotational ambiguity inherent to these pure component factorizations is reduced by considering only those concentration factors which are possible solutions of the kinetic equations for properly adapted reaction rate constants. To this end we introduce the set $\mathcal{K}$ of rate constants whose associated solutions of the kinetic equations result in feasible concentration factors. Further, the subset $\mathcal{K}^+$ of $\mathcal{K}$ is defined by taking only those reaction rate constants whose associated concentration factors C can be supplemented by nonnegative spectral factors A so that the product CA reconstructs the initial spectral observation matrix. Finally, the set $\mathcal{K}^+$ is extended to a set of feasible rate constants with respect to perturbations $\mathcal{K}^+_\varepsilon$ by introducing an accepted noise level $\varepsilon \geq 0$. A central result of this paper is a theorem which characterizes the set $\mathcal{K}$ by a similarity condition for the Kirchhoff matrix.

1.1. Organization of the paper

The paper is organized as follows: Section 2 recapitulates an elementary model example of the slow-fast ambiguity for a first-order consecutive reaction system with three components [16, 17]. Section 3 shows how a kinetic hard-model can be implemented by a cost function which depends only on the reaction rate constants. The central definitions of the sets of consistent and feasible reaction rate constants are introduced in Section 4. Additionally this section contains the central results of the paper, namely Theorem 4.3 on a simple characterization of consistent vectors of rate constants. Section 5 is devoted to an extension of the set of feasible reaction rate constants to noisy data. Finally, in Section 6 the new concepts are applied to various first-order reaction schemes. The associated sets of consistent and feasible reaction rate constants are mathematically derived and numerically computed.

2. Rate constants ambiguity for an elementary first-order consecutive reaction

The kinetic equation of a first-order chemical reaction with given initial concentrations c_0 has the form of the vectorial initial value problem

$$\frac{dc(t)}{dt} = M(k)\,c(t), \qquad c(t_1) = c_0. \tag{2.1}$$

Therein the $s \times s$ matrix $M(k)$ is the kinetic or Kirchhoff matrix and s is the number of chemical components. It depends on nonnegative reaction rate constants, which are written by a vector $k \in \mathbb{R}^q$ with q components.

A simple consecutive first-order reaction scheme with three components is sufficient in order to demonstrate a certain non-uniqueness of the reaction rate constants, which is known as the slow-fast ambiguity [16].

Example 2.1. *We consider the first order consecutive reaction*

$$X \xrightarrow{k_1} Y \xrightarrow{k_2} Z$$

with the initial concentrations $(1, 0, 0)$ *for X, Y and Z. The associated kinetic matrix or Kirchhoff matrix reads*

$$M(k) = \begin{pmatrix} -k_1 & 0 & 0 \\ k_1 & -k_2 & 0 \\ 0 & k_2 & 0 \end{pmatrix}. \tag{2.2}$$

The solution of the initial value problem (2.1) *for these initial concentrations and this Kirchhoff matrix with* $(k_1, k_2) = (2, 1)$ *results in concentration profiles which are shown in the first row of Figure 1. Additionally, this first row in Figure 1 shows the three pure component spectra which we have assumed. The associated series of mixture spectra, i.e. the rows of the matrix D, are plotted in Figure 2. A second set of rate constants, namely* $(\tilde{k}_1, \tilde{k}_2) = (1, 2)$*, exists, which is consistent with the spectral data matrix D. The resulting concentration profiles and pure component spectra are shown in the second row of Figure 1.*

This example problem allows to explain the slow-fast

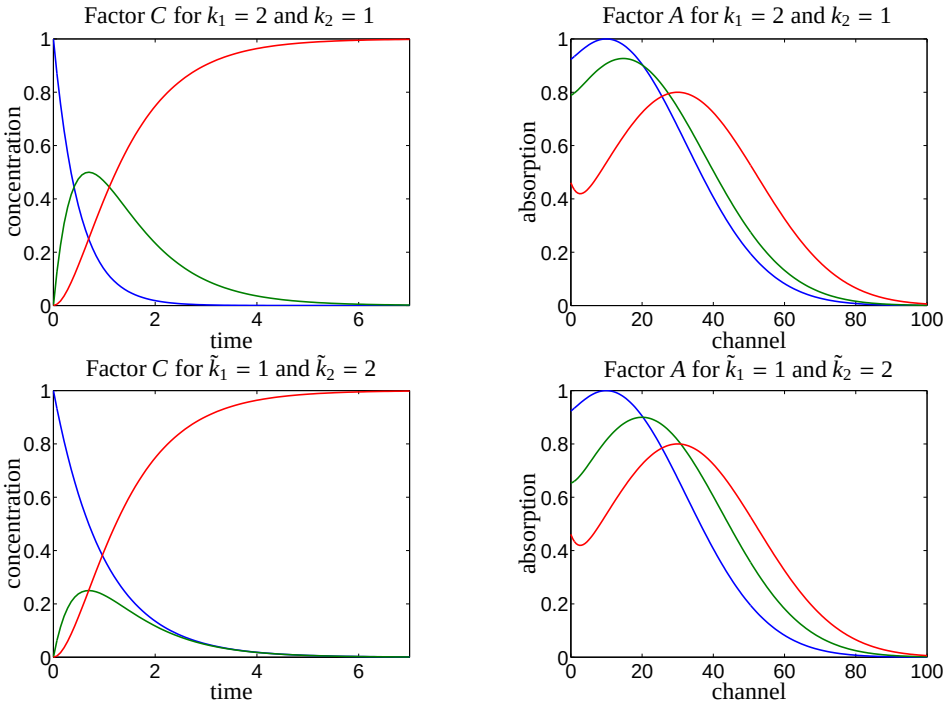

Figure 1: Two different factorizations for the consecutive reaction described in Example 2.1. The associated series of spectra for the mixture is shown in Figure 2. The two concentration factors are consistent with the kinetic model $X \xrightarrow{k_1} Y \xrightarrow{k_2} Z$ for different sets of kinetic rate constants. The factor A is nonnegative for each of these factorizations. Thus the two factorizations are feasible and consistent with the given kinetic model.

ambiguity [21, 16, 17]. The crucial point is that the two concentration profiles of the reaction product Z (in red color) in the left column in Figure 1 are identical even though the vectors of rate constants are different. In other words, if the concentration of Z is an observable quantity, then at least two sets of rate constants exist, which result in the same concentration profile.

3. Kinetic hard-modeling and pure component factorizations

We consider the following pure component factorization problem: For a given spectral data matrix $D \in \mathbb{R}^{m\times n}$ a factorization $D = CA$ is wanted with nonnegative factors $C \in \mathbb{R}^{m\times s}$ and $A \in \mathbb{R}^{s\times n}$. The spectral data matrix D contains in its m rows the mixture spectra taken at m times from a chemical reaction system. Each spectral profile contains absorption values at n frequencies. The number s represents the assumed active and independent chemical components. We understand an independent chemical component as a chemical component which increases the rank of the spectral data matrix D by 1. Thus s is the rank of the matrices D, C and A for noise-free and non-perturbed data. The matrices C and A contain the concentration profiles and spectra of the s pure components. For an introduction to this factorization problem see, e.g., [1] and the references therein. Usually, the nonnegative factorization $D = CA$ is not unique. Instead, continua of nonnegative matrices C and A exist. These sets of feasible solutions can be represented by the low-dimensional AFS plots.

We are interested in a chemically correct and interpretable factorization for which the s columns of the concentration factor C describe the concentration profiles of the s chemical components along the time axis. The associated factor A contains in its rows the pure component spectra. The a priori knowledge of a chemical reaction scheme is a very useful information in order to determine chemically relevant factorizations $D = CA$. In the best possible case only a single solution is consistent with the chemical reaction scheme. A by-product of such model-fit computations are optimally adapted reaction rate constants. In other cases, not only a single solution can be identified, but a small subset of the initial set of all nonnegative factorizations of D. With respect to the AFS representation of these solutions, such a subset can have the form of a one-dimensional curve within a two-dimensional AFS set

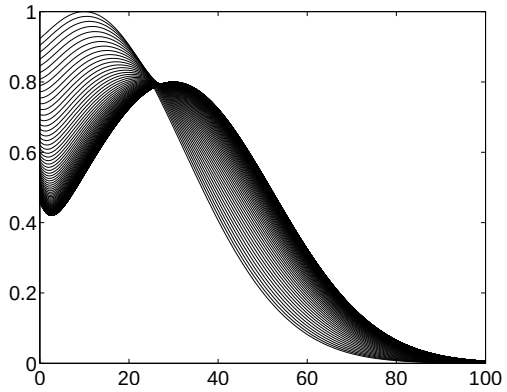

Figure 2: Series of mixture spectra for the three-component consecutive reaction $X \to Y \to Z$, see Example 2.1.

(for the case of a three-component system).

3.1. A cost function on nonnegativity and consistency with a kinetic hard-model

A certain chemical reaction scheme can be integrated into a pure component factorization $D = CA$. This often allows to reduce the rotational ambiguity drastically. This integration can be done in the form of a hard constraint by considering a proper cost functional within an SVD-based optimization procedure [1, 13, 22, 23]. Alternatively, the hard model approach can be combined with additional soft constraints in a joint optimization, see e.g. [15].

In the following, we use the hard model approach. This means that we construct a cost function $f(k)$ which depends only on the (unknown) vector $k \in \mathbb{R}^q$ of reaction rate constants. By solving the associated initial value problem (IVP), solely those concentration profiles are considered as possible factors $C = C^{(\mathrm{ode})}(k) \in \mathbb{R}_+^{m\times s}$ which fulfill the IVP (2.1) and for which an associated nonnegative spectral factor A exists so that CA approximates the given mixture data matrix D. Optimal values of the rate constants are computed by a numerical minimization of the cost function. We still have to explain how the time-continuous solution of the IVP

$$c(t) = \begin{pmatrix} c_1(t) \\ \vdots \\ c_s(t) \end{pmatrix} \in \mathbb{R}^s \tag{3.1}$$

is related to the matrix factor $C^{(\mathrm{ode})}(k) \in \mathbb{R}_+^{m\times s}$. This matrix results from an evaluation of the concentration functions along the time grid $t_1 < t_2 < \cdots < t_m$. Thus $C^{(\mathrm{ode})}(k)$ is completely determined by the vector of rate constants k. Finally, $D \approx U\Sigma V^T$ is a truncated singular value decomposition [24] with the rank s, which is the number of independent species. The numerical evaluation of the cost function for a given vector k is summarized in the steps:

1. $C^{(\mathrm{ode})}(k)$ is computed by solving the initial value problem (2.1).
2. The $s \times s$ matrix $T = (C^{(\mathrm{ode})}(k))^+ U\Sigma$ is computed with the pseudo-inverse $(C^{(\mathrm{ode})}(k))^+$ of $C^{(\mathrm{ode})}(k)$. (By the left-multiplication with the pseudo-inverse a least-squares problem is solved with respect to the s-dimensional column space of U.)
3. The matrix factors $C = U\Sigma T^{-1}$ and $A = TV^T$ are calculated.
4. The value of the cost function $f(k)$ is

$$\begin{aligned} f(k) = &\sum_{i=1}^{m}\sum_{j=1}^{s}\left(\min\left(\frac{C_{ij}}{\max_l(C_{lj})}, 0\right)\right)^2 \\ &+ \sum_{i=1}^{s}\sum_{j=1}^{n}\left(\min\left(\frac{A_{ij}}{\max_l(A_{il})}, 0\right)\right)^2 \\ &+ \|C^{(\mathrm{ode})}(k) - C\|_F^2. \end{aligned} \tag{3.2}$$

   Therein the squared Frobenius norm $\|\cdot\|_F^2$ is the sum of squares of its argument.

This approach is closely related to the pure hard-modeling of de Juan et al. in [13]. A minor difference is that we expand the time-discrete concentration with respect to the left singular values of D, which means no difference for model data and amounts to a low-rank approximation for perturbed data. In contrast to the well-known hard-soft MCR methods, the matrices C and A are completely determined by the $s \times s$ matrix T, which again is directly related to the matrix $C^{(\mathrm{ode})}(k)$, see steps 2 and 3 of the cost function. This underlines the high impact of the kinetic model on the pure component factors C and A.

For model data, which have been generated from a given kinetic model, no low-rank approximation is necessary as the data matrix has at most the rank s (aside from rounding errors). Then $\min_k f(k) = 0$ holds and the associated matrix $C^{(\mathrm{ode})}(k)$ coincides with the matrix C.

In general cases, additional vectors of rate constants $\tilde{k}$ can exist, which also fulfill $f(\tilde{k}) = 0$. In such cases, the kinetic model does not provide sufficient information in order to restrict the rotational ambiguity only to a single pure component factorization $D = CA$. Such ambiguities are well known for irreversible consecutive chemical reactions; cf. Example 2.1.

4. Parameter ambiguity for general first-order kinetics

The ambiguity of the reaction rate constants for general first-order reaction systems is analyzed in this section. The central result of this section is Theorem 4.3 which provides a simple criterion for determining sets of rate constants that are consistent with the factorization of the given spectral data.

4.1. Definitions of sets of consistent and feasible reaction rate constants

We assume that the given spectral data matrix $D \in \mathbb{R}^{m\times n}$ has at least one factorization $D = CA$ with nonnegative factors $C \in \mathbb{R}^{m\times s}$ and $A \in \mathbb{R}^{s\times n}$. Therein, the s columns of the concentration factor C should be interpreted as the concentration profiles of the s chemical components along the time axis. The m entries of each column of C are the concentration values for the points in time $t_1, \ldots, t_m$. Finally, we assume that the concentration factor C is consistent with a vector $k \in \mathbb{R}^q$ of nonnegative reaction rate constants in the following sense: The initial value problem (2.1) with the Kirchhoff matrix $M(k)$ has a solution $c(t) = (c_1(t), \ldots, c_s(t))^T \in \mathbb{R}^s$ so that the evaluation of these s concentration profiles for the points in time $t_1, \ldots, t_m$ reproduces the matrix factor C. Mathematically this evaluation with respect to the grid points $t_1, \ldots, t_m$ reads

$$C = \begin{pmatrix} c_1(t_1) & \ldots & c_s(t_1) \\ \vdots & & \vdots \\ c_1(t_m) & \ldots & c_s(t_m) \end{pmatrix} =: \mathcal{T}c(t). \tag{4.1}$$

The last equation defines the time grid discretization operator $\mathcal{T}$ which evaluates the time-continuous solution $c(t)$ of (2.1) on the given time grid. This results in the matrix C.

With these preparations we define the set of D-consistent rate constants as follows:

Definition 4.1 (Set of D-consistent reaction rate constants)**.** *Let $D = U\Sigma V^T$ be the singular value decomposition of the rank-s matrix $D \in \mathbb{R}^{m\times n}$. The set of D-consistent reaction rate constants $k \in \mathbb{R}^q$ is defined as*

$$\begin{aligned}\mathcal{K} = \{k \in \mathbb{R}^q : {} & c(t) \text{ solves (2.1), } C = \mathcal{T}c(t) \text{ and} \\ & \exists T \in \mathbb{R}^{s\times s}, \operatorname{rank}(T) = s \text{ and } C = U\Sigma T^{-1}\}.\end{aligned} \tag{4.2}$$

In words the set $\mathcal{K}$ of D-consistent rate constants comprises all reaction rate constants whose associated solution $c(t)$ of (2.1) on the discrete time grid $t_1, \ldots, t_m$ can be represented by the left singular vectors of D, i.e. the columns of U. (Sometimes we call the D-consistency simply consistency.)

This definition of the D-consistent rate constant is not sufficient to guarantee that the concentration factor C can be supplemented by a nonnegative spectral factor A in a way that the reconstruction $D = CA$ holds. This additional requirement is part of the following definition.

Definition 4.2 (Set of nonnegatively feasible rate constants)**.**

$$\begin{aligned}\mathcal{K}^+ = \{k \in \mathbb{R}^q : {} & c(t) \text{ solves (2.1), } C = \mathcal{T}c(t) \text{ and} \\ & \exists T \in \mathbb{R}^{s\times s}, \operatorname{rank}(T) = s, \; C = U\Sigma T^{-1} \\ & \text{with } A = TV^T \geq 0\}.\end{aligned} \tag{4.3}$$

The definition of the set $\mathcal{K}^+$, in comparison to (4.2), contains the additional demand that $A \geq 0$. Consequently it holds that $\mathcal{K}^+ \subseteq \mathcal{K}$. For the consecutive reaction from Example 2.1 the set of D-consistent reaction rate constants is equal to the set of nonnegatively feasible rate constants. This means that $\mathcal{K} = \mathcal{K}^+ = \{(2, 1), (1, 2)\}$.

4.2. Analysis by the eigenvalues of the Kirchhoff matrix

The set $\mathcal{K}$ of D-consistent rate constants can easily be characterized by the set of the eigenvalues of the kinetic matrix $M(k)$ in (2.1). Starting from a certain D-consistent rate constant vector $k^* \in \mathcal{K}$, a further vector k is also contained in $\mathcal{K}$ if $M(k^*)$ and $M(k)$ are similar matrices. (Similarity of $M(k)$ and $M(k^*)$ means that a regular matrix $Z \in \mathbb{R}^{s\times s}$ exists so that $M(k^*) = Z^{-1}M(k)Z$.) The following theorem contains the details.

Theorem 4.3. *Let $D \in \mathbb{R}^{m\times n}$ be a nonnegative matrix with $\operatorname{rank}(D) = s$ so that a matrix factorization $D = CA$ with $C \in \mathbb{R}^{m\times s}$ and $A \in \mathbb{R}^{s\times n}$ exists. For this D the*

vector $k^* \in \mathbb{R}^q$ is assumed to be a vector of D-consistent rate constants in the sense of Definition 4.1. This means that

$$\mathcal{T}\, c^*(t) = C^* = U\Sigma(T^*)^{-1} \tag{4.4}$$

with a regular $s \times s$ matrix T^*. Then the following equivalence holds:

The vector $k \in \mathbb{R}^q_+$ is D-consistent, if and only if the matrices $M(k)$ and $M(k^*)$ are similar matrices, i.e., they have the same sets of eigenvalues.

The proof of this theorem is postponed to Appendix A.

Remark 4.4. 1. *Theorem 4.3 shows that the set membership of a certain k to the set $\mathcal{K}$ of D-consistent reaction rate constants, see Definition 4.1, can simply be decided by testing the similarity of the matrices $M(k)$ and $M(k^*)$ with $k^* \in \mathcal{K}$. Similar matrices, this is written as $M(k) \sim M(k^*)$, have the same eigenvalues and their equal eigenvalues can be paired in a way that the associated eigenspaces have the same dimensions. (In the language of linear algebra, the sets of eigenvalues of $M(k)$ and $M(k^*)$ are the same and in the case of multiple eigenvalues any eigenvalue of $M(k)$ is associated with the same eigenvalue of $M(k^*)$ and these eigenvalues have the same geometric multiplicity, see [24].) With the similarity operator $\sim$ this can compactly be written as*

$$\mathcal{K} = \left\{ k \in \mathbb{R}^q : \; M(k) \sim M(k^*) \right\}. \tag{4.5}$$

2. *Numerically, Equation* (4.5) *can approximately be checked by the simple and computationally cheap computation of the sets of eigenvalues of $M(k)$ and $M(k^*)$. If $M(k)$ and $M(k^*)$ have equal eigenvalues (equality is meant with respect to a proper multiple of the machine precision) and if in the case of multiple eigenvalues all geometric multiplicities are the same, then $M(k) \sim M(k^*)$ holds. Numerically, the non-diagonalizabilty of a matrix (such a matrix is often called defective) cannot be checked as the Jordan normal form of a matrix cannot be computed numerically. The key point is that a proper arbitrarily small perturbation of a defective matrix can transform this matrix into a diagonalizable matrix (with a large condition number).*
3. *Theorem 4.3 provides a simple criterion on D-consistency in the sense of Definition 4.1. This criterion does not guarantee the nonnegativity of the factor A. If additionally the existence of a nonnegative factor A is required, then $\mathcal{K}$ reduces to its subset $\mathcal{K}^+$ of nonnegatively feasible rate constants.*

4.3. Graphical presentation of $\mathcal{K}$ and $\mathcal{K}^+$

If the first-order chemical reaction system is described by a number of q rate constants, then the sets $\mathcal{K}$ and $\mathcal{K}^+$ are subsets of the q-dimensional space. However only for $q = 2$ and $q = 3$ a graphical representation of these sets is easily possible by a 2D or 3D plot. Every opportunity should be taken in order to reduce the dimension of the graphical representation for the cases with $q \geq 4$. A reduction from the dimension q to $q - 1$ is possible in the following way:

1. Similar matrices have the same trace (sum of diagonal elements or, equivalently, sum of eigenvalues). Hence a constant ψ exists so that

$$\psi = -\sum_{i=1}^{q} \lambda_i = -\text{trace}(M(k)) \tag{4.6}$$

   for all $k \in \mathcal{K}$. The λ_i are the eigenvalues of $M(k)$.
2. For a first-order chemical reaction system the negative trace of the Kirchhoff matrix $M(k^*)$ with $k^* \in \mathcal{K}$ equals

$$\sum_{i=1}^{q} k_i = \psi$$

   as the ith subreaction contributes the term $-k_i$ to the diagonal of the Kirchhoff matrix $\mathcal{K}$; for an illustration of this relation see the example systems in Sections 6.2, 6.3 and 6.4.
3. A combination of the last two equations shows that the jth rate constant k_j for $j \in \{1, \ldots, q\}$ can be expressed as

$$k_j = \psi - \sum_{\substack{i=1 \\ i \neq j}}^{q} k_i \,. \tag{4.7}$$

Hence the linear relation (4.7) allows to present the sets $\mathcal{K}$ and $\mathcal{K}^+$ within a $(q-1)$-dimensional space.

4.4. Numerical computation of $\mathcal{K}$ and $\mathcal{K}^+$

The numerical computation of the set $\mathcal{K}$ of all vectors of D-consistent reaction rate constants, see Definition 4.1, requires very long computation times. For each possible k an initial value problem is to be solved in order to determine the matrix $C^{(\text{ode})}(k)$. The result of Theorem 4.3 is that initial value problems are not be solved any longer. Instead an eigenvalue problem is to be solved for the small $s \times s$ Kirchhoff matrix $M(k)$. This

is a simple and computationally very cheap step. Additionally, Section 4.3 shows that $\mathcal{K}$ can graphically be represented in a $(q-1)$-dimensional space. A straightforward strategy for the computation of $\mathcal{K}$ is a systematic grid search. Therefore we cover a proper bounded subset of the $\mathbb{R}^{q-1}$ by an equidistant grid. For each grid point, the grid points are vectors of rate constants, it is checked whether or not this point fulfills the D-consistency. A comparable grid search has been used in [25] for the computation of the area of feasible solutions.

The starting point for the grid search algorithm is a certain D-consistent rate constant k^*. Such an initial solution can be calculated by using a proper hard-modeling kinetic procedure as used in [13, 1]. Then the grid search can be started. For very simple reaction systems the whole computation can be done analytically, see Section 6 for an example. In the general case, a numerical approximation of $\mathcal{K}$ is the only practical approach.

Finally, the subset $\mathcal{K}^+$ of nonnegatively feasible rate constants can be extracted from $\mathcal{K}$ by checking computationally the nonnegativity of the factor A according to Definition 4.2.

4.5. Link to the area of feasible solutions

The area of feasible solutions (AFS), e.g. see [4, 5, 6, 7, 8, 9], represents the set of all factorizations $D = CA$ with nonnegative factors C and A for a given spectral data matrix D. In more detail, the concentrational AFS which is denoted by $\mathcal{M}_C$ in [7] is a low-dimensional representation of the set of all nonnegative factors C. Analogously, the spectral AFS $\mathcal{M}_A$ is a low-dimensional representation of all spectral factors A. The AFS is computed only by using the spectral data matrix D. The AFS does not include a consistency check of the nonnegative solutions in C and A with a kinetic model of the reaction. This fact opens the possibility to combine the information on the set of nonnegatively feasible rate constants $\mathcal{K}^+$ with the AFS construction. The feasibility condition by Definition 4.2 imposes an additional constraint on the areas of feasible solutions $\mathcal{M}_C$ and $\mathcal{M}_A$. Hence subsets of the AFS can be identified which represent those factorizations of D that are additionally consistent with the underlying kinetic model. In Section 6.7 and Figure 14 numerical results of such a combination of $\mathcal{M}_C$ and $\mathcal{M}_A$ with a kinetic model are presented.

An interesting additional feature of the set $\mathcal{K}^+$ is that the scaling information for the factors C and A is known as these factors result from the solution $C^{(\mathrm{ode})}$ of an initial value problem. All this provides the selected AFS solutions with an absolute scaling whenever a kinetic model of the reaction is accessible.

4.6. Application to data without sign restrictions

Up to now we have always assumed that the matrix D contains only nonnegative absorption data. However, Definition 4.1 of the set $\mathcal{K}$ describes the consistency with the kinetic model and does not require D to be a nonnegative matrix. At first, the analysis by the set $\mathcal{K}^+$ includes that the spectral factor A is a componentwise nonnegative matrix. Hence, any spectroscopic technique which underlies the bilinear Lambert-Beer law can be analyzed in the sense of the set $\mathcal{K}$. We have tested this for simulated circular dichroism spectroscopic data.

5. Computation of $\mathcal{K}^+$ for perturbed data

Section 4 contains an analysis of the ambiguity of the kinetic rate constants for first-order kinetics. Up to now this analysis is restricted to non-perturbed model data and cannot be applied to experimental data with a nonzero noise-to-signal ratio. For experimental data the minimum of the cost function $f(k)$, see Equation (3.2), is usually larger than zero. Hence the definition of the set of D-consistent rate constants $\mathcal{K}$ in Equation (4.2) cannot be applied in its strict sense, since the non-perturbed solution $C^{(\mathrm{ode})}$ of the initial value problem cannot precisely be reconstructed from the left singular vectors of D.

In order to overcome this problem and in order to analyze the sensitivity of the reaction rate constants, we define the set of feasible rate constants $\mathcal{K}_\varepsilon^+$ for a noise level whose magnitude is controlled by the parameter ε. The set $\mathcal{K}_\varepsilon^+$ contains all rate constants for which the cost function $f(k)$ from Equation (3.2) returns a value not larger than ε. The following algorithm for the computation of $\mathcal{K}_\varepsilon^+$ uses the set $\mathcal{K}$ as its starting point.

5.1. Definition of the set of feasible rate constants for perturbed data

The set of nonnegatively feasible rate constants $\mathcal{K}_\varepsilon^+$ with respect to the noise level $\varepsilon \geq 0$ is defined to be

$$\mathcal{K}_\varepsilon^+ = \{k \in \mathbb{R}_+^q : \ f(k) \leq \varepsilon\}. \tag{5.1}$$

Therein, the cost function $f(k)$ is given in (3.2). By the construction of f the inequality $f(k) \leq \varepsilon$ guarantees that negative entries of C and A are bounded from below and that $C^{(\mathrm{ode})}$ is re-constructable from the left singular vectors except for a minor error which tends to zero if

ε tends to zero. For the limit case $\varepsilon = 0$ it holds that $\mathcal{K}_0^+ = \mathcal{K}^+$.

For perturbed data the trace invariance property from Section 4.3 is no longer true. In other words $\sum_{i=1}^{q} \lambda_i$ is not constant in cases with $\varepsilon > 0$. Hence the representation of $\mathcal{K}^+$ for a system with q rate constants can only be given in the $\mathbb{R}_+^q$ and not in the $\mathbb{R}_+^{q-1}$.

5.2. Algorithmic approach for the computation of $\mathcal{K}_\varepsilon^+$

In Section 4 a strategy has been developed for the computation of $\mathcal{K}$ and $\mathcal{K}^+$. Based on the properties $\mathcal{K}^+ \subseteq \mathcal{K}$ and $\mathcal{K}^+ \subset \mathcal{K}_\varepsilon^+$ for any $\varepsilon > 0$ a procedure to compute $\mathcal{K}_\varepsilon^+$ is outlined next:

1. Starting from a D-consistent rate constant k^* (or at least the k^* which minimizes $f(\cdot)$) the associated set $\mathcal{K}$ is computed by the grid search algorithm.
2. The set $\mathcal{K}$ is reduced to $\mathcal{K}^+$ by testing the nonnegativity constraint for the factor A.
3. The set $\mathcal{K}^+$ is inflated to the set $\mathcal{K}_\varepsilon^+$ by evaluating the cost function f in a neighborhood of $\mathcal{K}^+$.

Steps 1 and 2 are explained in Section 4. Step 3 is described in the next subsection.

5.3. Numerical inflation of $\mathcal{K}^+$ to $\mathcal{K}_\varepsilon^+$

The set $\mathcal{K}_\varepsilon^+$ for $q = 2$ is planar and a subset of $\mathbb{R}_+^2$. Its numerical computation can be based on the same techniques as have been used for the computation of the area of feasible solutions in [4, 5, 6, 7]. In particular, these concepts are the grid search method [25], the triangle enclosure procedure [6] or the polygon inflation method [7, 8]. Minor changes in the program codes are necessary, namely the target function, which classifies a rate constant as feasible or not, has to be changed.

For the case $q = 3$ the set $\mathcal{K}_\varepsilon^+$ is a subset of $\mathbb{R}_+^3$. Once again, the grid search method, the sliced triangle enclosure procedure [26] or a polyhedron inflation algorithm are appropriate tools for the computation of $\mathcal{K}_\varepsilon^+$.

6. System analysis for model data sets and experimental data

In this section the analytical concepts are applied to four different sets of model data and additionally to one data set of experimental UV/Vis spectra. These demonstrations include the analysis of four different types of first-order chemical reactions which include consecutive reactions and equilibrium reactions. For the model data sets the ambiguity of the reaction rate constants are analyzed by computing the sets $\mathcal{K}$ and $\mathcal{K}^+$. For the UV/Vis data and also for two of the model data sets the sets $\mathcal{K}_\varepsilon^+$ are computed for different values of ε.

6.1. A two-component reversible reaction system

We consider the reaction mechanism of the two-component reversible system

$$X \underset{k_{-1}}{\overset{k_1}{\rightleftharpoons}} Y$$

with the initial values $c_X(0) = 1$ and $c_Y(0) = 0$. The Kirchhoff matrix reads

$$M(k) = \begin{pmatrix} -k_1 & k_{-1} \\ k_1 & -k_{-1} \end{pmatrix}.$$

The eigenvalues of $M(k)$ are $\lambda_1 = -k_1 - k_{-1}$ and $\lambda_2 = 0$.

The concentration profiles can be computed by solving the associated initial value problem. The reference reaction rate constants are taken as $k_1^* = 2$ and $k_{-1}^* = 1$. For this parametrization the concentration profiles are shown together with the associated pure component spectra, two Gaussian functions are assumed, in Figure 3.

First the set of D-consistent rate constants $\mathcal{K}$ is determined. Therefore all 2×2 matrices are to be determined which are similar to $M(k)$. By similarity these matrices have the eigenvalues $-k_1 - k_{-1}$ and 0. With the trace of a reference matrix $M(k^*)$ with $\psi = k_1^* + k_{-1}^*$, cf. Equation (4.6), this leads to the linear relation

$$k_1 + k_{-1} = \psi.$$

This equation describes a straight line in the positive quadrant of the positive rate constants. In other words $k_{-1} = \psi - k_1$. Hence

$$\mathcal{K} = \left\{ \begin{pmatrix} \alpha \\ \psi - \alpha \end{pmatrix} : \alpha \in (0, \psi] \right\}. \tag{6.1}$$

In order to determine the subset $\mathcal{K}^+$ we fix in the present model problem $k_1^* = 2$ and $k_{-1}^* = 1$ so that $\psi = 3$, cf. Equation (4.6). By an elimination in the equation $CA = \widetilde{C}\,\widetilde{A}$ which describes two feasible factorizations (for the details see [27]) we get the subset of rate constants $\mathcal{K}^+$ being associated with nonnegative A

$$\mathcal{K}^+ = \left\{ \begin{pmatrix} \alpha \\ \psi - \alpha \end{pmatrix} : \alpha \in [1.9004, \psi] \right\}. \tag{6.2}$$

Therein the lower bound for α satisfies

$$k_1 \max_{i=1,\ldots,n} \frac{A_{1i} - A_{2i}}{A_{1i}} = 1.9004.$$

The sets $\mathcal{K}$ and $\mathcal{K}^+$ as well as the associated continua of nonnegative factors C and A are shown in Figure 4.

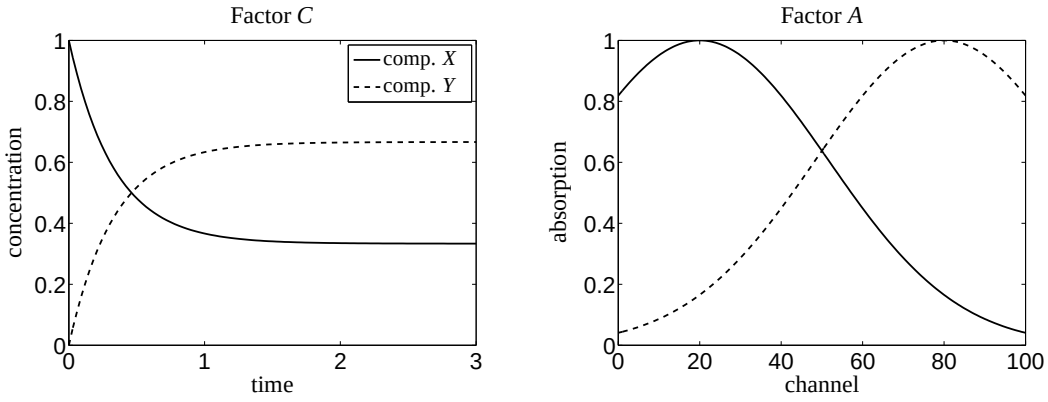

Figure 3: Concentration profiles and pure component spectra for the two-component model problem from Section 6.1.

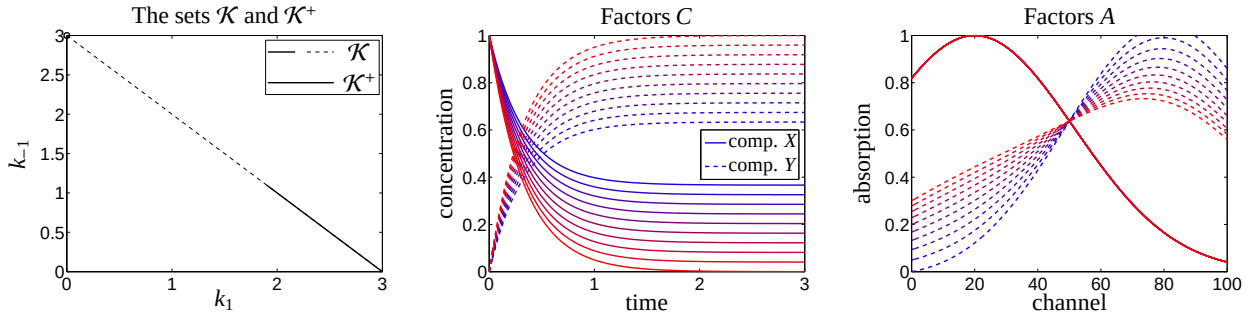

Figure 4: The model problem from Section 6.1 is considered. Left: The set of D-consistent rate constants $\mathcal{K}$ by (4.2) is an anti-diagonal broken line and solid line in $[0,3]\times[0,3]$. Its subset of nonnegatively feasible kinetics $\mathcal{K}^+$ by (4.3) is drawn as a solid line. These sets are analytically given in (6.1) and (6.2). The vector $k=(0,3)$ is not an element of $\mathcal{K}$; this open end of the set is marked by a small black circle.
Center and right: The continua of associated nonnegative factors C and A for the set of feasible kinetics $\mathcal{K}^+$ are plotted. A color shading from red to blue is used in order to express the pairing of associated concentration profiles and spectra. The isolated red spectral profile in the right subplot is the spectral profile of X, which can uniquely be extracted from the data at $t=0$.

Next the same model problem is considered for nonnegative initial concentrations values $c_X(0) > 0$ and $c_Y(0) > 0$. Then the subset $\mathcal{K}^+$ of $\mathcal{K}$ consists of two isolated line segments, see Figure 5.

6.2. A three-component partially reversible reaction system - part 1

The reaction mechanism for a three-component system is taken as follows

$$X \xrightarrow{k_1} Y \underset{k_{-2}}{\overset{k_2}{\rightleftharpoons}} Z.$$

The initial concentrations are given by $c_X(0) = 1$, $c_Y(0) = 0$ and $c_Z(0) = 0$, and the Kirchhoff matrix reads

$$M(k) = \begin{pmatrix} -k_1 & 0 & 0 \\ k_1 & -k_2 & k_{-2} \\ 0 & k_2 & -k_{-2} \end{pmatrix}.$$

The eigenvalues of the matrix $M(k)$ are $\lambda_1 = -k_1$, $\lambda_2 = -k_2 - k_{-2}$ and $\lambda_3 = 0$. For the model problem the reference values $k_1^* = 1$, $k_2^* = 2$ and $k_{-2}^* = 1$ are used. For these parameters the concentration profiles and the pure component spectra (three Gaussians) are presented in Figure 6.

The set of D-consistent rate constants $\mathcal{K}$ and its subset of feasible rate constants $\mathcal{K}^+$ have the following forms

$$\begin{aligned} \mathcal{K} &= \left\{ \begin{pmatrix} \phi \\ \alpha \\ \psi - \phi - \alpha \end{pmatrix} : \alpha \in (0, \psi - \phi] \right\} \cup \left\{ \begin{pmatrix} \psi - \phi \\ \beta \\ \phi - \beta \end{pmatrix} : \beta \in (0, \phi] \right\} \\ \mathcal{K}^+ &= \left\{ \begin{pmatrix} \phi \\ \alpha \\ \psi - \phi - \alpha \end{pmatrix} : \alpha \in [1.7155, \psi - \phi] \right\} \cup \\ &\qquad \left\{ \begin{pmatrix} \psi - \phi \\ \beta \\ \phi - \beta \end{pmatrix} : \beta \in [0.8087, \phi] \right\} \end{aligned} \tag{6.3}$$

with $\phi = k_1^* = 1$ and $\psi = k_1^* + k_2^* + k_{-2}^* = 4$. The lower bounds for α and β in $\mathcal{K}^+$ result from a numerical evaluation of the following terms

$$\begin{aligned} k_2 \max_{i=1,\dots,n} \frac{A_{2i} - A_{3i}}{A_{2i}} &= 1.7155, \\ k_1 \max_{i=1,\dots,n} \frac{(\psi - k_1)A_{1i} + (k_1 - k_{-2})A_{2i} - k_2 A_{3i}}{k_1 A_{2i} + (\psi - k_1)A_{1i}} &= 0.8087. \end{aligned}$$

The derivation of these formula requires complex mathematical computations which have been done by using computer algebra systems; all results have been confirmed numerically by means of the grid search procedure. The set $\mathcal{K}$ and its subset $\mathcal{K}^+$ of feasible rate constants are plotted in Figure 7. These sets can be plotted in 2D as the fixed trace condition, see Section 4.3, implies the linear relation $k_1 = \psi - k_2 - k_{-2}$ wherein the constant $\psi = 4$ is the sum of the components of $k^* = (1, 2, 1)$. Figure 7 additionally shows the continua of the concentration profiles and of the nonnegative spectra which are represented by $\mathcal{K}^+$.

6.3. A three-component partially reversible reaction system - part 2

As a second reaction mechanism for a three-component system we consider

$$X \underset{k_{-1}}{\overset{k_1}{\rightleftharpoons}} Y \xrightarrow{k_2} Z$$

with the initial concentrations $c_X(0) = 1$, $c_Y(0) = 0$ and $c_Z(0) = 0$. The Kirchhoff matrix is given by

$$M(k) = \begin{pmatrix} -k_1 & k_{-1} & 0 \\ k_1 & -k_{-1} - k_2 & 0 \\ 0 & k_2 & 0 \end{pmatrix}.$$

Its eigenvalues are $\lambda_{1,2} = -(\psi \pm \sqrt{\phi})/2$ and $\lambda_3 = 0$ with

$$\psi = k_1 + k_{-1} + k_2, \quad \phi = (k_1 + k_{-1} + k_2)^2 - 4k_1 k_2.$$

We use the reference values $k_1^* = 2$, $k_{-1}^* = k_2^* = 1$. The three pure component spectra for X, Y and Z are the same as used in Section 6.2, see Figure 6. The concentration profiles are presented in Figure 8.

The sets $\mathcal{K}$ and $\mathcal{K}^+$ have the form

$$\begin{aligned} \mathcal{K} &= \left\{ \begin{pmatrix} \alpha \\ \beta(\alpha) \\ \gamma(\alpha) \end{pmatrix} : \alpha \in \left[\frac{\psi - \sqrt{\phi}}{2}, \frac{\psi + \sqrt{\phi}}{2} \right] \right\}, \\ \mathcal{K}^+ &= \left\{ \begin{pmatrix} \alpha \\ \beta(\alpha) \\ \gamma(\alpha) \end{pmatrix} : \alpha \in \left[1.3001, \frac{\psi + \sqrt{\phi}}{2} \right] \right\}. \end{aligned} \tag{6.4}$$

Therein the functions $\beta(\alpha)$ and $\gamma(\alpha)$ are given by

$$\beta(\alpha) = -\frac{1}{4} \frac{(\psi - 2\alpha)^2 - \phi}{\alpha}, \quad \gamma(\alpha) = \psi - \alpha - \beta(\alpha)$$

with $\psi = 4$, $\phi = 8$ and the given values for $k_{\pm 1}^*$ and k_2^*. The lower bound for α in $\mathcal{K}^+$ has the form

$$k_1 \max_{i=1,\dots,n} \frac{A_{1i} - A_{2i}}{A_{1i}} = 1.3001.$$

All these results together with the continua of nonnegative factors C and A which are represented by the set $\mathcal{K}^+$ of feasible rate constants are presented in Figure 9.

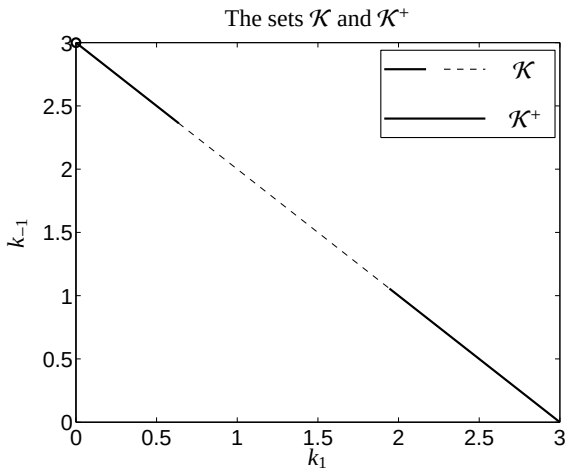

Figure 5: The model problem from Section 6.1 is considered for the case of nonnegative initial concentrations $c_X(0) = 0.55$ and $c_Y(0) = 0.45$. Once again the set of D-consistent rate constants $\mathcal{K}$ and also the set of feasible rate constants $\mathcal{K}^+$ are shown. The set $\mathcal{K}^+$ consists of two isolated line segments.

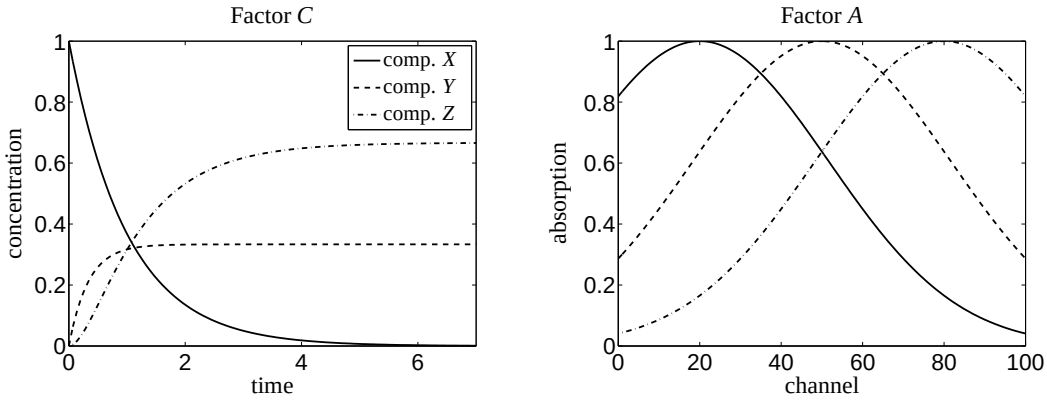

Figure 6: Concentration profiles and spectra of the pure components for the model problem from Section 6.2. The reaction rate constants are $k_1 = 1$, $k_2 = 2$ and $k_{-2} = 1$, and the initial concentrations are set to $c_X(0) = 1$, $c_Y(0) = 0$ and $c_Z(0) = 0$.

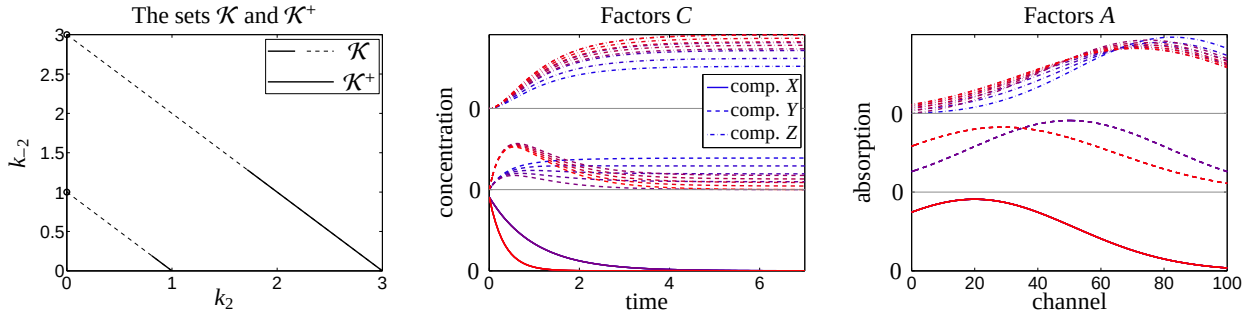

Figure 7: Analysis of the three-component model system from Section 6.2. Left: The set of D-consistent rate constants $\mathcal{K}$ is drawn by dashed and by solid lines. Its subset $\mathcal{K}^+$ is plotted by the solid line. All these lines are open at $k_2 = 0$, i.e. the points $(k_1, k_2, k_{-2}) = (3, 0, 1)$ and $(k_1, k_2, k_{-2}) = (1, 0, 3)$ do not belong to $\mathcal{K}$. These two points are marked by small circles. Because of the fixed trace condition, see Section 4.3, and $k_1 = 4 - k_2 - k_{-2}$ for $k^* = (1, 2, 1)$, the sets $\mathcal{K}$ and $\mathcal{K}^+$ can be drawn in 2D.
Center and right: The continua of associated nonnegative factors C and A for the set of feasible kinetics $\mathcal{K}^+$ are plotted. A color shading from red to blue is used in order to express the pairing of associated concentration profiles and spectra. The single/isolated concentration profiles or spectra represent unique solutions, e.g. the spectral profile of X can uniquely be extracted from the data at $t = 0$.

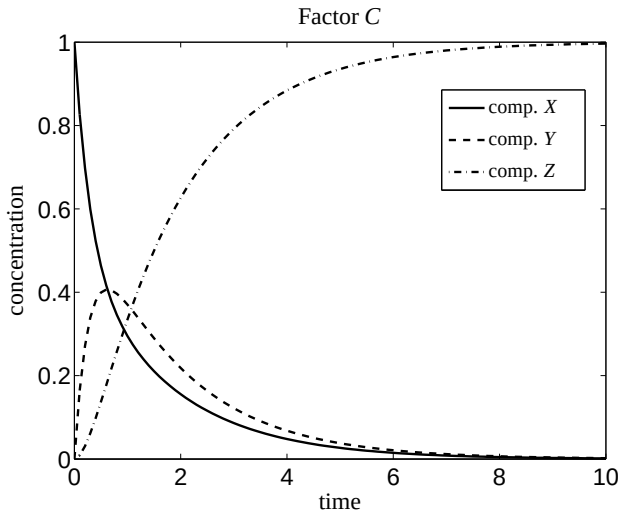

Figure 8: The concentration profiles for the three-component model system from Section 6.3. The pure component spectra are the same as used in Section 6.2 and are shown in Figure 6.

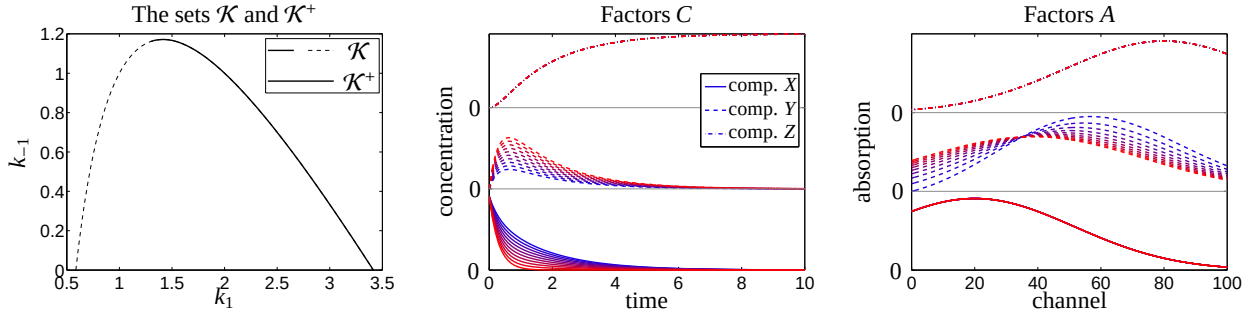

Figure 9: Analysis of the three-component model system from Section 6.3. Left: The set of D-consistent rate constants $\mathcal{K}$ is drawn by dashed and by solid curved lines. Its subset $\mathcal{K}^+$ is plotted by the solid line. These sets are given analytically in Equation (6.4). Because of the fixed trace condition, see Section 4.3, and $k_2 = 4 - k_1 - k_{-1}$, the sets $\mathcal{K}$ and $\mathcal{K}^+$ can be drawn in 2D.
Center and right: The continua of associated nonnegative factors C and A are plotted for the set of feasible kinetics $\mathcal{K}^+$. A color shading from red to blue is used in order to express the pairing of associated concentration profiles and spectra. The pure component spectra of X and Z are known (from the spectral data at $t = 0$ and $t = 10$). Then the complementarity theory [28, 29, 30] guarantees that the concentration profile of the complementary component Y is also uniquely determined aside from scaling; and in fact, the continuum of concentration profiles of Y is spanned by a single function and its scalar multiples.

6.4. A three-component system including parallel reactions

Next the three components X, Y and Z are assumed to form two reaction pathways for the component X. The reaction mechanism is

$$X \underset{k_{-1}}{\overset{k_1}{\rightleftharpoons}} Y, \quad X \xrightarrow{k_2} Z$$

with the initial concentrations $c_X(0) = 1$, $c_Y(0) = 0$ and $c_Z(0) = 0$. Hence the Kirchhoff matrix reads

$$M(k) = \begin{pmatrix} -k_1 - k_2 & k_{-1} & 0 \\ k_1 & -k_{-1} & 0 \\ k_2 & 0 & 0 \end{pmatrix}.$$

The eigenvalues of $M(k)$ are $\lambda_{1,2} = -(\psi \pm \sqrt{\phi})/2$, $\lambda_3 = 0$ with

$$\begin{aligned} \psi &= k_1 + k_{-1} + k_2, \\ \phi &= (k_1 + k_{-1} + k_2)^2 - 4k_{-1}k_2. \end{aligned}$$

The reference values for the rate constants are taken as $k_1^* = 2$ and $k_{-1}^* = k_2^* = 1$. Once again, the same Gauss profiles as used in Section 6.2 are taken for the pure component spectra. The solution of the initial value problem (2.1) with the present $M(k)$ and the given initial values results in the concentration profiles which are shown in Figure 10.

The set of D-consistent rate constants $\mathcal{K}$ and its subset of nonnegatively feasible rate constants $\mathcal{K}^+$ read

$$\begin{aligned} \mathcal{K} &= \left\{ \begin{pmatrix} \alpha(\beta) \\ \beta \\ \gamma(\beta) \end{pmatrix} : \beta \in \left[\frac{\psi - \sqrt{\phi}}{2}, \frac{\psi + \sqrt{\phi}}{2} \right) \right\}, \\ \mathcal{K}^+ &= \left\{ \begin{pmatrix} \alpha(\beta) \\ \beta \\ \gamma(\beta) \end{pmatrix} : \beta \in [0.58115,\ 1.7207] \right\}. \end{aligned} \tag{6.5}$$

Therein the constants $\alpha(\beta)$ and $\gamma(\beta)$ are given by

$$\alpha(\beta) = -\frac{1}{4}\frac{(\psi - 2\beta)^2 - \phi}{\beta}, \quad \gamma(\beta) = \psi - \alpha(\beta) - \beta$$

and $\psi = 4$, $\phi = 12$. The analytic formula for the β-interval in $\mathcal{K}^+$ are skipped due to their high complexity. Instead, only the numerical evaluation of these bounds is given. Figure 11 shows the sets $\mathcal{K}$ and $\mathcal{K}^+$ together with the associated continua of nonnegative feasible factors C and A.

6.5. Feasible rate constants for perturbed/noisy experimental data

Next the set of feasible rate constants is computed for UV/Vis data from [31] where the influence of substituents in ButiPhane ligands is investigated on the hydrogenation activity of rhodium complexes. A number of $k = 82$ UV/Vis spectra each with $n = 1951$ channels is given. The underlying reaction mechanism is simply $X \xrightarrow{k_1} Y$. In order to demonstrate the computation of the set of feasible rate constants we assume the slightly more complex mechanism of the equilibrium

$$X \underset{k_{-1}}{\overset{k_1}{\rightleftharpoons}} Y.$$

The set of nonnegatively feasible rate constants $\mathcal{K}_\varepsilon^+$ with respect to the noise level $\varepsilon \geq 0$ is computed, cf. (5.1). The following analysis allows to judge of the question whether or not the experimental data could also be interpreted by an equilibrium reaction.

Due to the high quality of the UV/Vis spectral data only a relatively small noise level ε is assumed. For the given experimental data we have observed the minimum $\min_k f(k) = 1.09 \cdot 10^{-5}$. This shows that ε must be larger than $1.09 \cdot 10^{-5}$ in order to find any feasible solutions. First the function $f(k)$ is evaluated on the rectangle of reaction rate constants

$$(k_1, k_{-1}) \in [10^{-3},\ 2 \cdot 10^{-2}] \times [0,\ 10^{-2}].$$

The results and the computed sets $\mathcal{K}_\varepsilon^+$ for the three different values $\varepsilon \in \{1.5 \cdot 10^{-3},\ 5 \cdot 10^{-3},\ 1 \cdot 10^{-2}\}$ are presented in Figure 12. All computations have been executed by using a simple grid search method; the computational costs for the evaluation of the cost function are not very high. As the set $\mathcal{K}_\varepsilon^+$ consists only of one connected set, even the polygon inflation technique [7] can be used for the numerical computation of $\mathcal{K}_\varepsilon^+$.

6.6. Numerical computation of the set $\mathcal{K}_\varepsilon^+$

In Section 5.1 the set $\mathcal{K}_\varepsilon^+$ of feasible rate constants for perturbed data is introduced. By definition it holds that

$$\mathcal{K}^+ \subset \mathcal{K}_\varepsilon^+ \subseteq \mathcal{K}_{\tilde{\varepsilon}}^+$$

for every $0 \leq \varepsilon \leq \tilde{\varepsilon}$.

First, we consider Example 2.1 for which the set $\mathcal{K}^+$ consists of only two isolated points. For the two noise levels

$$\varepsilon \in \{1 \cdot 10^{-3},\ 5 \cdot 10^{-3}\}$$

the two sets $\mathcal{K}_{\tilde{\varepsilon}}^+$ increase around $\mathcal{K}^+$, which is shown in the upper left sub-plot of Figure 13. For this problem

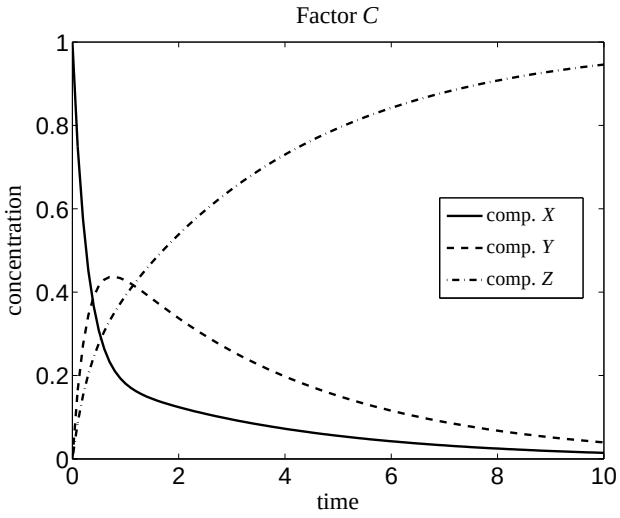

Figure 10: The concentration profiles for the three-component model data from Section 6.4. The pure component spectra are the same as used in Section 6.2 and shown in Figure 6.

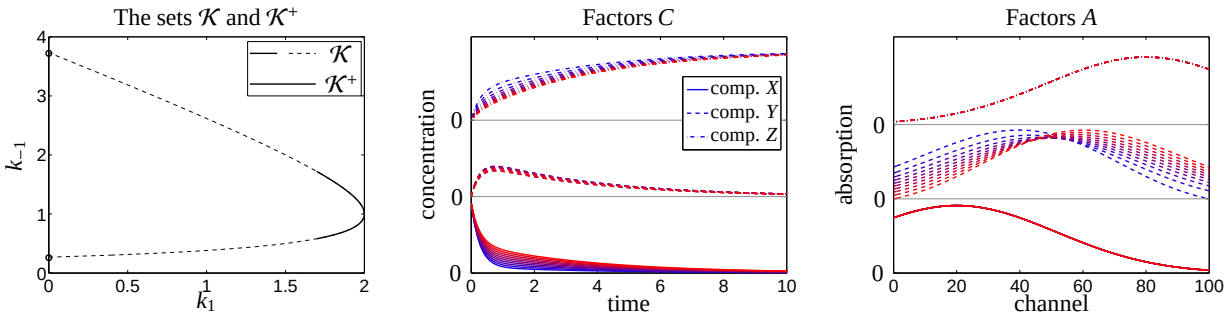

Figure 11: Analysis of the three-component model system including parallel reactions from Section 6.4. Left: The set of D-consistent rate constants $\mathcal{K}$ is drawn by dashed and by solid lines. Its subset $\mathcal{K}^+$ is plotted by the solid line. Because of the fixed trace condition, see Section 4.3, and $k_2 = 4 - k_1 - k_{-1}$ for $k^* = (2, 1, 1)$, the sets $\mathcal{K}$ and $\mathcal{K}^+$ can be drawn in 2D.
Center and right: The continua of associated nonnegative factors C and A for the set of feasible kinetics $\mathcal{K}^+$ are plotted. A color shading from red to blue is used in order to express the pairing of associated concentration profiles and spectra. The single/isolated spectra represent unique solutions.

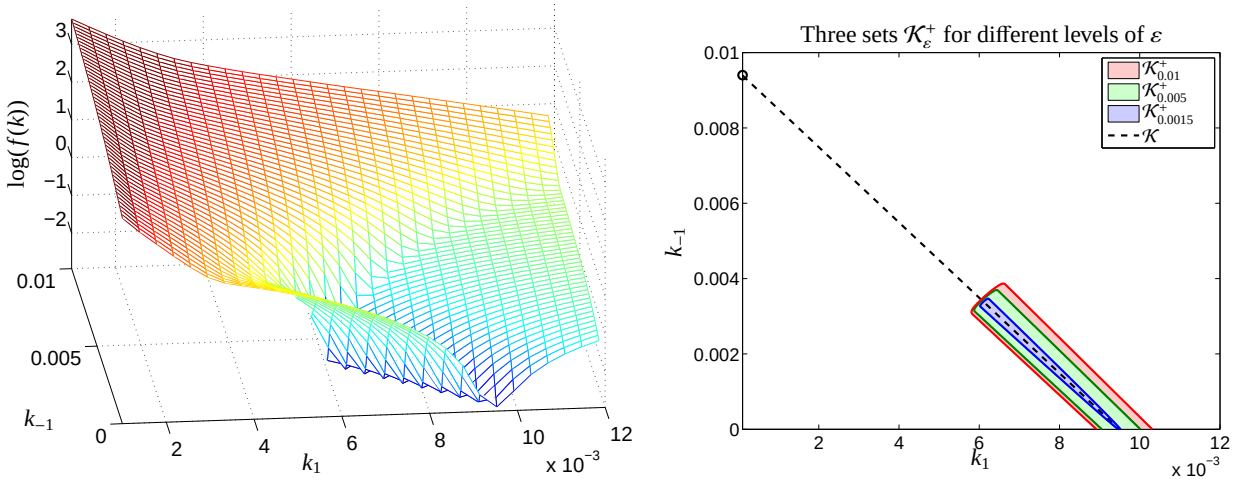

Figure 12: Analysis of the UV/Vis data set for ButiPhane ligands and the hydrogenation activity, see Section 6.5.
Left: Numerical evaluation of the cost function $f(k)$, see Equation (3.2).
Right: Different levels of ε lead to a chain of sets $\mathcal{K}_\varepsilon^+$. The three values $\varepsilon \in \{1.5 \cdot 10^{-3}, 5 \cdot 10^{-3}, 1 \cdot 10^{-2}\}$ have been used.

the two isolated solutions are transformed by noise to two continua of possible solutions. The upper right subplot of Figure 13 shows the set $\mathcal{K}^+$ for the reversible two-component reaction system from Section 6.1. For this experiment the three noise levels are

$$\varepsilon \in \{5 \cdot 10^{-5}, 5 \cdot 10^{-4}, 5 \cdot 10^{-3}\}.$$

The remaining two plots in the lower row of Figure 13 demonstrate the sets $\mathcal{K}^+$ and $\mathcal{K}_\varepsilon^+$ for the three-component model problem from Section 6.3 whose associated sets $\mathcal{K}$ and $\mathcal{K}^+$ are shown in Figure 9. In all these cases one observes a continuous effect of an increasing ε (i.e. small deviations from the kinetic model are accepted and also small negative entries in the factors C and A of the factorization $D = CA$ are accepted) on increasing sets $\mathcal{K}_\varepsilon^+$ of nonnegatively feasible reaction rate constants.

6.7. Combination of the AFS and $\mathcal{K}^+$

In Section 4.5 an explanation is given how the area of feasible solutions $\mathcal{M}$ can be combined with the set of feasible rate constants $\mathcal{K}^+$. Next a numerical example is given for the three-component model system from Section 6.4. Therefore the area $\mathcal{M}_C$ of feasible concentration factors C and the area $\mathcal{M}_A$ of feasible spectral factors A are plotted in Figure 14. Then the subset of all these AFS segments which represent solutions that belong to feasible rate constant vectors $\mathcal{K}^+$ in the sense of Definition 4.2 are marked by black color. This clearly indicates how strongly the consistency of a nonnegative factorization of D with an underlying kinetic model can reduce the rotational ambiguity. The series of the extracted concentrational factors and spectra are shown in Figure 11.

7. Conclusion

Kinetic modeling is widely used in the process of extracting pure component information from spectroscopic data. However, little attention is paid to the existence of an ambiguity of the rate constants. For first-order reaction schemes we have presented the theoretical basis together with an algorithmic approach for an efficient numerical computation of this ambiguity. Analytical investigations of these ambiguities have been carried out for four typical first-order reaction schemes. Additionally, numerical results have been presented for model data and UV/Vis experimental data. The latter results confirm the stability of the numerical algorithm with respect to noise.

References

[1] M. Maeder and Y.M. Neuhold. *Practical data analysis in chemistry*. Elsevier, Amsterdam, 2007.

[2] E. Malinowski. *Factor analysis in chemistry*. Wiley, New York, 2002.

[3] R. Tauler. Calculation of maximum and minimum band boundaries of feasible solutions for species profiles obtained by multivariate curve resolution. *J. Chemom.*, 15(8):627–646, 2001.

[4] O.S. Borgen and B.R. Kowalski. An extension of the multivariate component-resolution method to three components. *Anal. Chim. Acta*, 174:1–26, 1985.

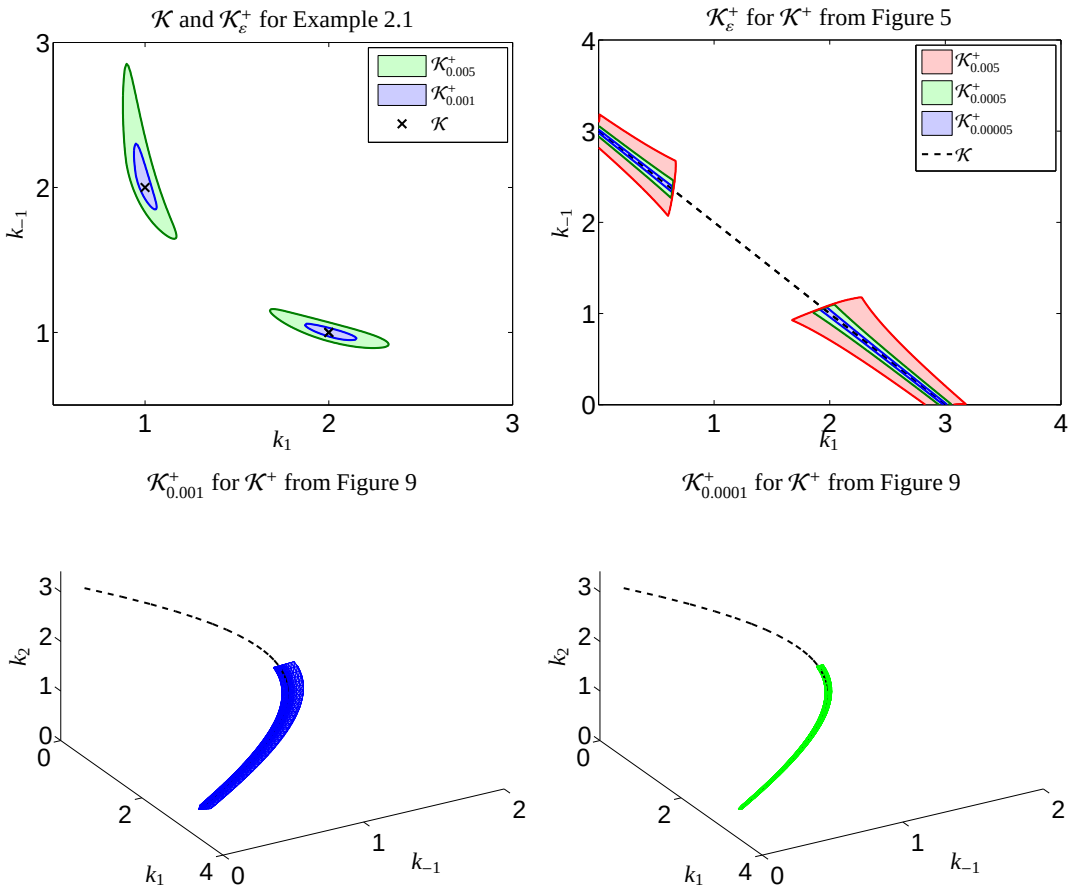

Figure 13: Numerical study of the impact of an increasing noise level ε on the sets $\mathcal{K}_\varepsilon^+$.
Upper left: For the data set from Example 2.1 the two-point set $\mathcal{K}^+$ increases to the two continua of possible solutions $\mathcal{K}_\varepsilon^+$ due to the two noise-levels $\varepsilon \in \{1 \cdot 10^{-3}, 5 \cdot 10^{-3}\}$.
Upper right: For the two-component model problem from Section 6.1 the set $\mathcal{K}^+$ shown in Figure 5 increases to the three sets $\mathcal{K}_\varepsilon^+$ for the three noise-levels $\varepsilon \in \{5 \cdot 10^{-5}, 5 \cdot 10^{-4}, 5 \cdot 10^{-3}\}$.
Lower row: For the three-component model problem from Section 6.3 the set $\mathcal{K}^+$ is shown in Figure 9. For a noise level $\varepsilon > 0$ the dimension reduction from $\mathbb{R}^3$ to $\mathbb{R}^2$ does not hold any longer so that the curvilinear set $\mathcal{K}^+$ inflates to tubular sets $\mathcal{K}_\varepsilon^+$ for $\varepsilon = 10^{-3}$ and $\varepsilon = 10^{-4}$. The crosses or dashed/solid black lines represent in all these cases the underlying sets $\mathcal{K}$ as shown in Figure 5 and Figure 9.

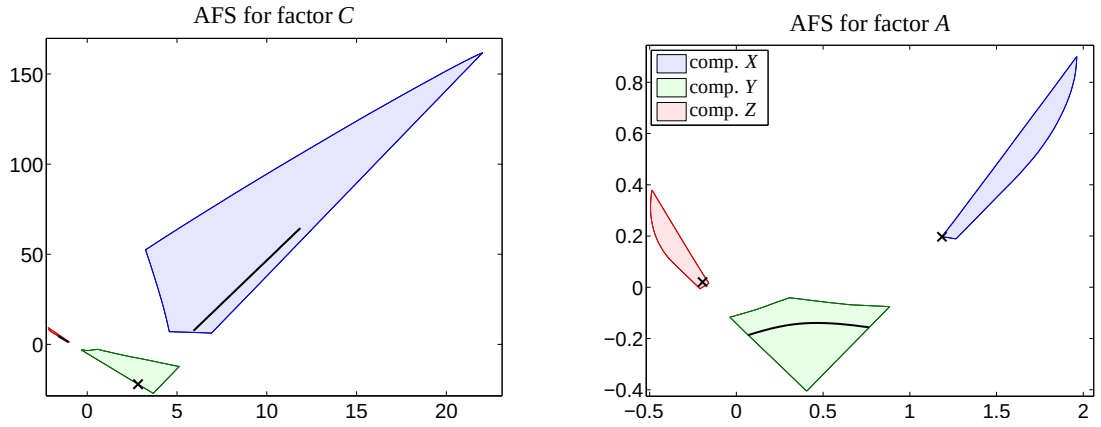

Figure 14: The areas of feasible solutions $\mathcal{M}_C$ and $\mathcal{M}_A$ for the three-component model problem from Section 6.4. The black points and curves are the low dimensional representations of the kinetic solutions $C^{(\mathrm{ode})}(k)$, $k \in \mathcal{K}^+$, and of the corresponding absorption factors. These factors are also plotted in Figure 11.

[5] R. Rajkó and K. István. Analytical solution for determining feasible regions of self-modeling curve resolution (SMCR) method based on computational geometry. *J. Chemom.*, 19(8):448–463, 2005.

[6] A. Golshan, H. Abdollahi, and M. Maeder. Resolution of Rotational Ambiguity for Three-Component Systems. *Anal. Chem.*, 83(3):836–841, 2011.

[7] M. Sawall, C. Kubis, D. Selent, A. Börner, and K. Neymeyr. A fast polygon inflation algorithm to compute the area of feasible solutions for three-component systems. I: Concepts and applications. *J. Chemom.*, 27:106–116, 2013.

[8] M. Sawall and K. Neymeyr. A fast polygon inflation algorithm to compute the area of feasible solutions for three-component systems. II: Theoretical foundation, inverse polygon inflation, and FAC-PACK implementation. *J. Chemom.*, 28:633–644, 2014.

[9] A. Jürß, M. Sawall, and K. Neymeyr. On generalized Borgen plots. I: From convex to affine combinations and applications to spectral data. *J. Chemom.*, 29(7):420–433, 2015.

[10] S. Beyramysoltan, H. Abdollahi, and R. Rajkó. Newer developments on self-modeling curve resolution implementing equality and unimodality constraints. *Anal. Chim. Acta*, 827(0):1–14, 2014.

[11] N. Rahimdoust, M. Sawall, K. Neymeyr, and H. Abdollahi. Investigating the effect of constraints on the accuracy of the area of feasible solutions in the presence of noise with an improved cost function of the polygon inflation algorithm; soft versus hard constrained SMCR. Accepted for J. Chemom., 2016.

[12] M. Sawall, N. Rahimdoust, C. Kubis, H. Schröder, D. Selent, D. Hess, H. Abdollahi, R. Franke, Börner A., and K. Neymeyr. Soft constraints for reducing the intrinsic rotational ambiguity of the area of feasible solutions. *Chemom. Intell. Lab. Syst.*, 149, Part A:140–150, 2015.

[13] A. de Juan, M. Maeder, M. Martínez, and R. Tauler. Combining hard and soft-modelling to solve kinetic problems. *Chemom. Intell. Lab. Syst.*, 54:123–141, 2000.

[14] J. Jaumot, P. J. Gemperline, and A. Stang. Non-negativity constraints for elimination of multiple solutions in fitting of multivariate kinetic models to spectroscopic data. *J. Chemom.*, 19(2):97–106, 2005.

[15] M. Sawall, A. Börner, C. Kubis, D. Selent, R. Ludwig, and K. Neymeyr. Model-free multivariate curve resolution combined with model-based kinetics: Algorithm and applications. *J. Chemom.*, 26:538–548, 2012.

[16] W. G. Jackson, J. M. Harrowfield, and P. D. Vowles. Consecutive, irreversible first-order reactions. Ambiguities and practical aspects of kinetic analyses. *Int. J. Chem. Kinet.*, 9(4):535–548, 1977.

[17] N.W. Alcock, D.J. Benton, and P. Moore. Kinetics of Series First-Order Reactions. *Trans. Faraday Soc.*, 66:2210–2213, 1970.

[18] W. O. Milligan, D. F. Mullica, D. E. Pennington, C. K. C. Lok, and D. W. J. Kwong. Application of nonlinear least squares analysis on three different consecutive irreversible first order kinetic proceses. *Comput. Chem. (Oxford)*, 8(4):285–298, 1984.

[19] S. Vajda and H. Rabitz. Identifiability and distinguishability of first-order reaction systems. *J. Phys. Chem.*, 92(3):701–707, 1988.

[20] S. Vajda and H. Rabitz. Identifiability and Distinguishability of General Reaction Systems. *J. Phys. Chem.*, 98(20):5265–5271, 1994.

[21] K.A. Connors. *Chemical kinetics*. VCH Publishers, Weinheim, 1990.

[22] S. Bijlsma and A. K. Smilde. Application of curve resolution based methods to kinetic data. *Anal. Chim. Acta*, 396:231–240, 1999.

[23] S. Bijlsma and A.K. Smilde. Estimating reaction rate constants from a two-step reaction: a comparison between two-way and three-way methods. *J. Chemom.*, 14(5-6):541–560, 2000.

[24] G.H. Golub and C.F. Van Loan. *Matrix Computations*. Johns Hopkins Studies in the Mathematical Sciences. Johns Hopkins University Press, Baltimore, MD, 2012.

[25] M. Vosough, C. Mason, R. Tauler, M. Jalali-Heravi, and M. Maeder. On rotational ambiguity in model-free analyses of multivariate data. *J. Chemom.*, 20(6-7):302–310, 2006.

[26] A. Golshan, M. Maeder, and H. Abdollahi. Determination and visualization of rotational ambiguity in four-component systems. *Anal. Chim. Acta*, 796(0):20–26, 2013.

[27] H. Schröder. Kinetische Modellierung für multivariate Faktormethoden. Master's thesis, University of Rostock, Mathematical institute, 2013.

[28] M. Sawall, C. Fischer, D. Heller, and K. Neymeyr. Reduction of the rotational ambiguity of curve resolution techniques under partial knowledge of the factors. Complementarity and coupling

theorems. *J. Chemom.*, 26:526–537, 2012.
[29] M. Sawall, C. Kubis, R. Franke, D. Hess, D. Selent, A. Börner, and K. Neymeyr. How to apply the complementarity and coupling theorems in MCR methods: Practical implementation and application to the Rhodium-catalyzed hydroformylation. *ACS Catal.*, 4:2836–2843, 2014.
[30] M. Sawall and K. Neymeyr. On the area of feasible solutions and its reduction by the complementarity theorem. *Anal. Chim. Acta*, 828:17–26, 2014.
[31] C. Fischer, S. Schulz, H.-J. Drexler, C. Selle, M. Lotz, M. Sawall, K. Neymeyr, and D. Heller. The Influence of Substituents in Diphosphine Ligands on the Hydrogenation Activity and Selectivity of the Corresponding Rhodium Complexes as Exemplified by ButiPhane. *ChemCatChem*, 4(1):81–88, 2012.

A. Appendix: Proof of the Theorem 4.3

This section contains the proof of the Theorem 4.3 from Section 4, which is a main result of this paper.

Proof. Let $c(t)$ and $c^*(t)$ be solutions of the initial value problems

$$\frac{dc(t)}{dt} = M(k)\,c(t), \qquad c(t_1) = c_0,$$
$$\frac{dc^*(t)}{dt} = M(k^*)\,c^*(t), \qquad c^*(t_1) = c_0.$$

We set the starting time t_1 equal to 0. This assumption does not restrict the generality of the proof as the zero point in time can be fixed arbitrarily. However, this allows us to write the solutions of the initial value problems in the simple form

$$c(t) = e^{M(k)t}c_0, \qquad c^*(t) = e^{M(k^*)t}c_0.$$

We assume the similarity $M(k) = Z^{-1}M(k^*)Z$ with a regular matrix $Z \in \mathbb{R}^{s\times s}$. We also assume that $M(k)$ and $M(k^*)$ are diagonalizable matrices; at the end of the proof the general case is treated. With the time-grid discretization operator from (4.1) we can write $C = C(k)$ as follows:

$$\begin{aligned} C = \mathcal{T}c(t) &= \begin{pmatrix} (c(t_1))^T \\ \vdots \\ (c(t_m))^T \end{pmatrix} \\ &= \begin{pmatrix} (e^{M(k)t_1}c_0)^T \\ \vdots \\ (e^{M(k)t_m}c_0)^T \end{pmatrix} \\ &= \begin{pmatrix} c_0^T(e^{Z^{-1}M(k^*)Zt_1})^T \\ \vdots \\ c_0^T(e^{Z^{-1}M(k^*)Zt_m})^T \end{pmatrix} \\ &= \begin{pmatrix} c_0^TZ^T(e^{M(k^*)t_1})^TZ^{-T} \\ \vdots \\ c_0^TZ^T(e^{M(k^*)t_m})^TZ^{-T} \end{pmatrix} \end{aligned}$$

with $Z^{-T} := (Z^{-1})^T$. Together with the diagonalization of $M(k^*) = Y^{-1}\Lambda Y$ for the diagonal matrix $\Lambda = \mathrm{diag}(\lambda_1, \ldots, \lambda_s)$ containing the eigenvalues $\lambda_1, \ldots, \lambda_s$, we continue the calculation from above

$$\begin{aligned} &= \begin{pmatrix} c_0^T(YZ)^Te^{\Lambda t_1}(YZ)^{-T} \\ \vdots \\ c_0^T(YZ)^Te^{\Lambda t_m}(YZ)^{-T} \end{pmatrix} \\ &= \begin{pmatrix} (YZc_0)^Te^{\Lambda t_1} \\ \vdots \\ (YZc_0)^Te^{\Lambda t_m} \end{pmatrix}(YZ)^{-T}. \end{aligned} \tag{A.1}$$

With the definition $w := YZc_0 \in \mathbb{R}^s$ the $(m \times s)$-matrix (in large brackets) in (A.1) can be written as

$$\begin{pmatrix} w^Te^{\Lambda t_1} \\ \vdots \\ w^Te^{\Lambda t_m} \end{pmatrix} = \begin{pmatrix} w_1e^{\lambda_1 t_1} & \ldots & w_se^{\lambda_s t_1} \\ \vdots & & \vdots \\ w_1e^{\lambda_1 t_m} & \ldots & w_se^{\lambda_s t_m} \end{pmatrix}. \tag{A.2}$$

The s column vectors

$$(e^{\lambda_i t_1}, \ldots, e^{\lambda_i t_m})^T \in \mathbb{R}^m$$

for $i = 1, \ldots, s$ span the column space of the matrix in Equation (A.2). In order to see that these two spaces are s-dimensional, one has to take into account that D, C and C^* are rank-s matrices.
We introduce the vector $w^* = Yc_0 \in \mathbb{R}^s$ in order to build

the matrix

$$\begin{pmatrix} (w^*)^T e^{\Lambda t_1} \\ \vdots \\ (w^*)^T e^{\Lambda t_m} \end{pmatrix} = \begin{pmatrix} w_1^* e^{\lambda_1 t_1} & \dots & w_s^* e^{\lambda_s t_1} \\ \vdots & & \vdots \\ w_1^* e^{\lambda_1 t_m} & \dots & w_s^* e^{\lambda_s t_m} \end{pmatrix}. \quad \text{(A.3)}$$

If w^* has no zero components (i.e. the rank-s condition), then the column spaces of (A.2) and (A.3) are the same and a regular $s \times s$ matrix G exists so that

$$\begin{pmatrix} w^T e^{\Lambda t_1} \\ \vdots \\ w^T e^{\Lambda t_m} \end{pmatrix} = \begin{pmatrix} (w^*)^T e^{\Lambda t_1} \\ \vdots \\ (w^*)^T e^{\Lambda t_m} \end{pmatrix} G.$$

With these results we continue the chain of transformations from Equation (A.1). Hence

$$\begin{aligned} C &= \begin{pmatrix} (YZc_0)^T e^{\Lambda t_1} \\ \vdots \\ (YZc_0)^T e^{\Lambda t_m} \end{pmatrix} (YZ)^{-T} = \begin{pmatrix} w^T e^{\Lambda t_1} \\ \vdots \\ w^T e^{\Lambda t_m} \end{pmatrix} (YZ)^{-T} \\ &= \begin{pmatrix} (w^*)^T e^{\Lambda t_1} \\ \vdots \\ (w^*)^T e^{\Lambda t_m} \end{pmatrix} G(YZ)^{-T} \\ &= \begin{pmatrix} c_0^T Y^T e^{\Lambda t_1} \\ \vdots \\ c_0^T Y^T e^{\Lambda t_m} \end{pmatrix} Y^{-T} Y^T G(YZ)^{-T} \\ &= \begin{pmatrix} c_0^T (e^{M(k^*)t_1})^T \\ \vdots \\ c_0^T (e^{M(k^*)t_m})^T \end{pmatrix} Y^T G(YZ)^{-T} \\ &= (\mathcal{T} c^*(t))\, Y^T G(YZ)^{-T} \\ &= C^*\, Y^T G(YZ)^{-T} \qquad \text{with (4.4)} \\ &= U\Sigma \underbrace{(T^*)^{-1} Y^T G(YZ)^{-T}}_{=:T^{-1}}). \end{aligned}$$

This is just the D-consistency of k with the regular $s \times s$ matrix $T^{-1} = (T^*)^{-1} Y^T G(YZ)^{-T}$.

The second direction of the proof can be shown by using the same arguments as used above. However, a partially new arrangement of the logical flow and of some of the definitions (e.g. of the matrix Z) is required. Further, the uniqueness of the solution of an initial value problem is used.

If the similar matrices $M(k)$ and $M(k^*)$ are not diagonalizable, then a continuity argument can be used to prove the assertion. The set of diagonalizable matrices is a dense set in the set of all matrices. In other words, arbitrarily small perturbations of a non-diagonalizable matrix can convert these into diagonalizable matrices. A continuity argument helps to transfer the assertion to the "small" set of non-diagonalizable matrices. □